The variational formulation of brittle fracture: numerical implementation and extensions

B. Bourdin

Department of Mathematics, Louisiana State University, Baton Rouge, LA 70803, USA (bourdin@math.lsu.edu)

Summary. This paper presents the implementation of a variational formulation of brittle fracture mechanics proposed by G.A. Francfort and J.-J. Marigo in 1998. The essence of the model relies on successive global minimizations of an energy with respect to any crack set and any kinematically admissible displacement field. We briefly present the model itself, and its variational approximation in the sense of Gamma–convergence. We propose a globally convergent and monotonically decreasing numerical algorithm. We introduce a backtracking algorithm whose solution satisfy a global optimality criterion with respect to the time evolution. We illustrate this algorithm with three dimensional numerical experiments. Then we present an extension of the model to crack propagation under thermal load and its numerical application to the quenching of glass.

Key words: Variational Model, Brittle Fracture, Crack Path Identification, Free Discontinuity Model, Gamma Convergence

Introduction

The work presented here is based an original approach proposed by G. Francfort and J.-J. Marigo in [18, 19]. While this model is still limited to quasi-static problems under fixed displacement boundary conditions, we extend it to account for body forces under some restrictions. The main virtue of the model we use is to remain largely compatible with Griffth theory, departing as little as possible to allow crack initiation or branching, path identification, and interactions between multiple cracks. However, these benefits have a cost in terms of complexity of the numerical implementation. The Francfort-Marigo formulation involves a *global* minimization of a total energy with respect to *any* admissible crack set and displacement field, and requires specialized numerical tools which we present in this article.

1 Francfort and Marigo's model for quasi-static brittle fracture

The brittle fracture formulation studied in this paper was first introduced by G. Francfort and J.J. Marigo, see [18, 17, 16, 12, 13] for a comprehensive presentation of the model. We will only briefly recall the essential points of this approach. As the emphasis of this paper is on the numerical implementation, we limit ourselves to a time discrete formulation. The reader will refer to [17, 16] for the time-continuous limit of the model. We differ from the original in that we consider body forces (under some restrictions) while the original formulation is restricted to fixed displacement boundary conditions.

In all that follows, we consider a two or three dimensional body with reference configuration $\Omega \subset \mathbb{R}^N$ $(N = 1, 2, 3)$ open, bounded with Lipschitz boundary. We assume that Ω can be partitioned into two connected subdomains Ω_F and Ω_D, corresponding respectively to a *fragile* and *ductile* materials with Hooke's law $\mathrm{A_F}$ and $\mathrm{A_D}$. We suppose that a part $\Omega_{D,0} \subset \Omega_D$ with non-null measure is clamped while $\partial\Omega \setminus \partial\Omega_{D,0}$ remains traction free.

The first key ingredient of the Francfort-Marigo model is to identify the cracks of the brittle material with the discontinuities of the displacement field. For that matter, we consider displacement fields in the space of Special Functions of Bounded Deformations (SBD). A detailed presentation of the space SBD is far beyond the scope of this article, the key point here is that any function $u \in SBD$ may be discontinuous, and that one can define its discontinuity set (or jump set) J_u.

We consider $P + 1$ time steps $0 \leq t^{(0)} < ... < t^{(P)} = T$. At each time step $t^{(p)}$, we apply a force $f(t^{(p)}; x)$ on Ω_D. In the sequel, we will assume that f depends linearly on t, that is that $f(t; x) := t.f(x)$.

The set of kinematically admissible displacement fields is

$$\mathcal{K}_A^{(p)} := \left\{ u \in SBD(\Omega)\,;\, u(x) = 0 \text{ a.e. in } \Omega_{D,0}\,;\, J_u \subset \bar{\Omega}_F\,;\, \|u\|_\infty \leq M \right\}, \quad (1)$$

where M is an arbitrarily large constant whose role is purely technical. Again we will refer the reader to [18, 17] for a complete exposition of the model.

In order to account for the *irreversible* nature of the fracture process, we define the *total* jump set at time step p of a sequence $\left(u^{(0)}, \ldots, u^{(P)}\right)$ by

$$\Gamma_u^{(p)} := \bigcup_{0 \leq s \leq p} J_{u^{(s)}}. \quad (2)$$

Note that we have trivially that $\Gamma_u^{(s)} \subset \Gamma_u^{(p)}$ for any $s \leq p$ so that the total crack set indeed grows monotonically.

The second key of Francfort Marigo is the *global minimization* of a total energy with respect to *any* admissible displacement field. For that, we define the bulk, surface, and total energies by

$$E^b(u(t^{(p)})) := \frac{1}{2}\int_{\Omega_F} \mathrm{A_F}\mathbf{e}(u) : \mathbf{e}(u)\, dx + \frac{1}{2}\int_{\Omega_D} \mathrm{A_D}\mathbf{e}(u) : \mathbf{e}(u) \; - 2f \cdot u\, dx, \tag{3}$$

$$E^s(u(t^{(p)})) := \gamma \mathcal{H}^{N-1}(\Gamma_u^{(p)}), \tag{4}$$

$$E(u(t^{(p)})) := E^b(u(t^{(p)})) + E^s(u(t^{(p)})), \tag{5}$$

where $\mathcal{H}^{N-1}$ denotes the $N-1$–dimensional Hausdorff measure (*i.e.* the length in two dimensions and surface in the three dimensional case), $\mathbf{e}(u)$ denotes the symmetrized gradient of u, and γ is the fracture toughness of the brittle material considered. At time $t^{(p)}$, the displacement field $u(t^{(p)})$ is solution of the *global minimization problem*:

$$\inf_{u \in \mathcal{K}_A^{(p)}} E(u), \tag{6}$$

and will denote by $E(t^{(p)})$ the total energy $E(u(t^{(p)}))$. Similarly, by $E^s(t^{(p)})$ and $E^b(t^{(p)})$, we refer to the surface and bulk energy of the solution of (6).

As the crack set at time t is given through a global minimization process among all possible crack states, the Francfort-Marigo model does not require *a priori* knowledge of the crack path. It does not even require the existence of an initial crack. It also does not assume smooth propagation of cracks (*i.e.* that the surface energy $E_s(t)$ is a continuous function of t). Indeed, as we will see in the numerical experiments, it is often the case that the total crack length is a discontinuous function of the time, a phenomenon we will refer to as *brutal* crack propagation.

2 Numerical implementation

In order to discretize the Francfort-Marigo functional, one needs to be able to approximate *any* function in SBD. This is by nature more complicated that building a discrete space allowing jumps across a known curve or surface. For that reason, the extended finite elements method is not easily applicable. This model also requires the ability to accurately approximate the location of the cracks, as well as their *length*, which may not be possible if the cracks are restricted to propagate along edges of faces in between elements like in a discontinuous Galerkin or cohesive finite element methods, for instance. Lastly, in light of [14], it is expected that in absence of singularity in the deformation field, cracks initiation will always be brutal. In particular, this means that sensitivity with respect to "small" cracks will never provide a descent direction toward a global minimizer of the Francfort-Marigo energy, in the case of "brutal" crack evolution.

Several methods have been proposed, based on discontinuous (see [21]) or adaptive (see [9, 24]) finite elements. Our previous experience with adaptive

finite elements is that the mesh adaption step can introduce artificial local minimizers and render the global minimization of E_ε practically impossible. The method which we present here relies on approximating the Francfort-Marigo energy, in the sense of Γ–convergence, by means of elliptic functionals. It is similar to the one proposed in [3, 4] for the Mumford-Shah functional, inspired by a now classical example in phase transition by [22, 23, 2] and extended in [6, 12, 13, 20].

2.1 Approximation of the Francfort-Marigo energy

Following [3, 4], we introduce a secondary variable $v \in W^{1,2}(\Omega)$, representing the crack in some sense, and for any $\varepsilon > 0$, $\eta_\varepsilon = o(\varepsilon)$, and $\alpha_\varepsilon = o(\varepsilon)$, we define

$$E_\varepsilon(u,v) := E^b_\varepsilon(u,v) + E^s_\varepsilon(v) := \frac{1}{2}\int_{\Omega_F} \left(v^2 + \eta_\varepsilon\right) \mathrm{A_F}\mathbf{e}(u) : \mathbf{e}(u)\, dx$$
$$+ \frac{1}{2}\int_{\Omega_D} \mathrm{A_D}\mathbf{e}(u) : \mathbf{e}(u) \, - 2f\cdot u\, dx + \gamma \int_\Omega \frac{(1-v)^2}{4\varepsilon} + \varepsilon|\nabla v|^2\, dx. \quad (7)$$

We do not attempt to prove the Γ–convergence of E_ε to E here. However, it is a known result in the original setting of the Francfort-Marigo model (*i.e.* when considering fixed displacement boundary conditions) and does not seem to be difficult to adapt to this case (see [10, 12, 13, 20]). Using a classical compactness argument (see for instance [15, 11]), one obtains that the global minimizers of $(u^\varepsilon, v^\varepsilon)$ of E_ε converge to that of E, and that in some weak sense, the set $\{x \in \Omega\,;\, v^\varepsilon(x) \le \alpha_\varepsilon\}$ converges to J_u.

In order to account for the irreversibility, we define

$$K^{(p)}_\varepsilon := \left\{ x \in \bar{\Omega}\ ;\ v^{(p)} \le \alpha_\varepsilon \right\}. \quad (8)$$

At each time step, we seek for $\left(u^{(p)}_\varepsilon, v^{(p)}_\varepsilon\right)$ solution of the problem

$$\begin{cases} \inf & E_\varepsilon(u,v). \\ u \in \mathcal{K}^{(p)}_A & \\ v = 0 \text{ on } K^{(p)}_\varepsilon. & \end{cases} \quad (9)$$

The last step in view of the numerical implementation of Francfort and Marigo's brittle fracture model is its discretization. For the Mumford-Shah problem, one can consider a discretized version $F_{\varepsilon,h}$ of F_ε by means of linear finite elements. Provided that the mesh size h is such that $h \ll \varepsilon$, it is known that $F_{\varepsilon,h}$ Γ–converges to F (see [5, 7]). Extending this result to our case does not seem to present any difficulty but is again not the scope of this study. We will take for granted that the restriction $F_{\varepsilon,h}$ of F_ε to discrete functions on a linear finite element space Γ–converges to F. This relation between the mesh

size and the regularization parameter can be an issue. However, a careful study of the Γ–convergence results in [5, 7] reveal that the relation $h \ll \varepsilon$ needs only to be verified "close" to the cracks. Unfortunately, finding the location of the cracks is the essence of the problem! In the numerical results we present, we used uniformly fine meshes, which can result very large meshes (typically, 10,000 to 50,000 elements in two dimensions and 200,000 to 1,500,000 elements in three dimensions).

2.2 Minimization methods

A major hurdle in the way of the minimization of (7) is its non-convexity. However, it is easy to see that E_ε is convex with respect to each of its arguments *separately*, and can therefore be iteratively minimized with respect to u and v. In the experiments presented later we used the following alternate minimization algorithm, δ being a fixed tolerance parameter:

Algorithm 1 *The alternate minimization algorithm*

Let $i = 0$ *and* $v_0 := v_\varepsilon^{(p-1)}$ *if* $p > 0$ *or* $v_0 = 1$ *if* $p = 0$.
repeat
  $i \leftarrow i + 1$
  Compute $u_i := \operatorname{argmin}_u F_\varepsilon(u, v_{i-1})$ *with* $u_i = 0$ *on* $\Omega_{D,0}$.
  Compute $v_i := \operatorname{argmin}_v F_\varepsilon(u_i, v)$ *under the constraint* $v_i = 0$ *on* $K_\varepsilon^{(p-1)}$
until $\|v_i - v_{i-1}\|_\infty \leq \delta$
Set $u_\varepsilon^{(p)} := u_i$ *and* $v_\varepsilon^{(p)} := v_i$

It can be proved (see [8]) that in cases where the crack propagation is smooth, this algorithm converges to the global minimizer, provided that the time discretization is fine enough. In cases where cracks propagate brutally, this algorithm can only be proved to converge to a critical point of E_ε, which may be a local (or a global) minimizer, but also a saddle point for E_ε. In some cases, the local minimizers of E_ε can be proved to converge to local minimizers of E, but no such a thing can be said of its saddle points.

A full treatment of saddle points would require studying the stability of critical points, and has not been implemented yet. In order to detect some saddle points and local minimizers, we implemented a backtracking in time algorithm, based on necessary condition for optimality of the crack evolution with respect to time. In the sequel, we assume that the boundary condition grows linearly with time, *i.e.* that $g(t; x) := tg(x)$. If this is the case, it is easy to see that if $(u^{(p)}, v^{(p)})$ is admissible for E_ε at time step $t^{(p)}$, then for any $0 \leq r \leq p$, $\left(\frac{t^{(r)}}{t^{(p)}} u^{(p)}, v^{(p)}\right)$ is admissible for $t^{(r)}$. Noticing then that $E_\varepsilon^b\left(\frac{t^{(r)}}{t^{(p)}} u^{(p)}, v^{(p)}\right) = \left(\frac{t^{(r)}}{t^{(p)}}\right)^2 E_\varepsilon^b(u^{(p)}, v^{(p)})$, we see that if $u^{(r)}$ and $u^{(p)}$ are global minimizers of E at time steps $t^{(r)}$ and $t^{(r)}$, then one necessarily has that

$$E_\varepsilon(u^{(r)}, v^{(r)}) \leq \left(\frac{t^{(r)}}{t^{(p)}}\right)^2 E^b_\varepsilon(u^{(p)}, v^{(p)}) + E^s_\varepsilon(v^{(p)}), \text{ for any } 0 \leq r \leq p. \quad (10)$$

In order to ensure that condition (10) is satisfied at each time step, we implemented the following backtracking algorithm, δ_ε being a small tolerance parameter:

Algorithm 2 *The backtracking algorithm*

1: $v_0 \leftarrow 1$
2: ***repeat***
3: *Compute* $(u^{(p)}, v^{(p)})$ *using the alternate minimization algorithm initialized with* v_0.
4: *Compute the bulk energy* $E^b_\varepsilon(u^{(p)}, v^{(p)})$ *and the surface energy* $E^s_\varepsilon(u^{(p)}, v^{(p)})$
5: ***for*** $r = 1$ *to* $p - 1$ ***do***
6: ***if*** $E_\varepsilon(u^{(r)}, v^{(r)}) - \left(\frac{t^{(r)}}{t^{(p)}}\right)^2 E^b_\varepsilon(u^{(p)}, v^{(p)}) - E^s_\varepsilon(v^{(p)}) \geq \delta_\varepsilon$ ***then***
7: $v_0 \leftarrow v^{(p)}$
8: $p \leftarrow r$
9: ***return*** *to 3:*
10: ***end if***
11: ***end for***
12: $v_0 \leftarrow v^{(p)}$
13: $p \leftarrow p + 1$
14: ***until*** $p = P$

3 Numerical Experiments

We present some numerical experiments based on the formulation and algorithms presented above. We consider a three dimensional cylinder of radius 2 and length 10, along the z–axis reinforced in its center by a ductile shaft of radius .5 (depicted in light grey in Figure 1) capped at each end by a rigid reinforcement (in black in Figure 1). The elastic moduli of both materials are $E = 1$ and $\nu = .2$, while the fracture toughness is normalized to $\gamma = 1$. The bottom cap is clamped while on the top one, a body force is applied along the positive z direction. On the brittle material, we initiated a hairline crack along a disk of radius .4 centered at the edge of the outer cylinder, and forming an angle of 30 degrees with the xy–plane.

The domain is meshed using 130,950 nodes and 584,150 linear tetrahedral elements. The magnitude of the force varies linearly between .5 and 5.5 in 250 time steps.

Figure 2 represent the evolution of the total and surface energies between the times $t = 1.4$ and $t = 1.9$. The location of the crack set at various times is shown in Figure 3. In these figures, the part of the domain corresponding to the britle material has been removed, and the ductile reinforcement is transparent. The upper and lower rows of figures correspond to the same

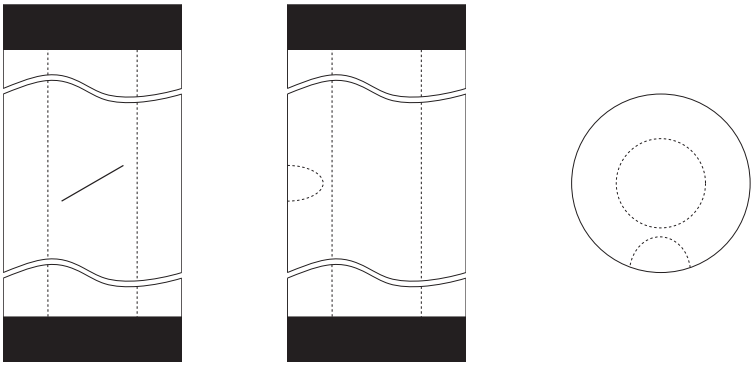

Fig. 1. Computational domain. Front, side and top views

time steps seen from different angles. The crack is represented by plotting the iso-volume $v \leq 5.0\text{E} - 2$.

The outcome of the alternate minimizations, combined with the backtracking is as follows:

- For $0 \leq t \leq 1.76$, no crack appears, however, the numerical solution exhibits some spurious surface energy (the lower branch of the dotted curve on Figure 2–right).
- At $t = 1.7$, the minimization algorithm bifurcates towards a cracked solution, and the surface energy jumps from 2.48 to 6.49. However, the total energy jumps from -12.5 to -14.2, which is forbidden by (10). The algorithm backtracks then to $t = 1.5$, time of the first violation of (10).
- Restarting from $t = 1.5$, alternate minimization lead to a smooth propagation of the crack until $t = 1.82$.
- At $t = 1.84$, the minimization algorithm bifurcates again towards a solution with an helicoidal crack. Again, the total energy jumps, which is in contradiction with (10), and the algorithm backtracks to $t = 1.64$
- At $t \geq 1.64$, the crack continue to grow, this time along the interface separating the fiber and the matrix (two rightmost figures in Figure 3). The evolution is smooth and the surface energy is continuous.

The final evolution can be summarized as follows:

- For $0 \leq t \leq 1.50$, no crack appears.
- At $t = 1.5$, a crack appears brutally starting from the existing notch (see Figure 3–left). The surface energy jumps (see the first jump of the plain curve in Figure 2–right).
- This crack propagates slowly for $1.50 \leq t \leq 1.62$ (see the slow growth of the plain curve in Figure 2–right) until it reaches the configuration in Figure 3 (second from the left).
- At $t = 1.64$, the crack propagates brutally again along a helicoidal path (Figure 3 center). The surface energy jumps again (second jump of the

plain curve in Figure 2–right). The crack spreads along the entire width of the brittle part, from the reinforcement until the edge of the matrix.
- For $t > 1.64$, a second branch of the crack develops along the reinforcement–matrix interface.

The total final and surface energy are represented by the plain lines in Figure 2. Using the backtracking algorithm, the total energy is continuous, (which is mandated by (10)), while solutions obtained without backtracking can enjoy discontinuities (see [24] Figure 11 or [10] Section 3.2). While we can still not guaranty that our solution corresponds to a global minimizer of the Francfort-Marigo energy, its energty is certainly less that that of a solution obtained without backtracking step (which would correspond to the upper envelope of the dashed curve in Figure 2–left).

This experiment also illustrates another strength of the Francfort-Marigo model and of our implementation. Recall again that in this experiment, the crack path (which is far from obvious) was not not known *a priori*. Using the Francfort-Marigo model, we were able to compute the crack path, as well as the position of the crack along this path. By using the approximation in the sense of Γ–convergence, we were able to represent complicated geometries. Note how the branch growing along the interface and the helix crack merge at $t = 3.08$. One of the virtue of our representation of the crack set is that it allows for such complicated change of topology without any special numerical treatment.

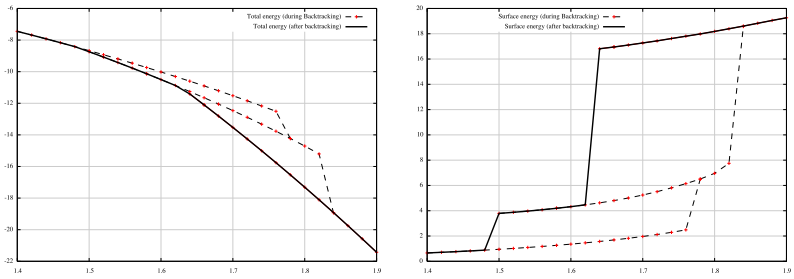

Fig. 2. Total and surface energy as a function of the load

4 Extensions to thermal loads

We present here some preliminary results on the extension of the Francfort-Marigo model to thermal loads.

In all that follows, we consider a *given* temperature field $\theta(t; x)$. In doing so, we assume that a thermal analysis of the problem can be made *a priori*, and in particular we neglect the effect of the cracks on the thermal conductivity of

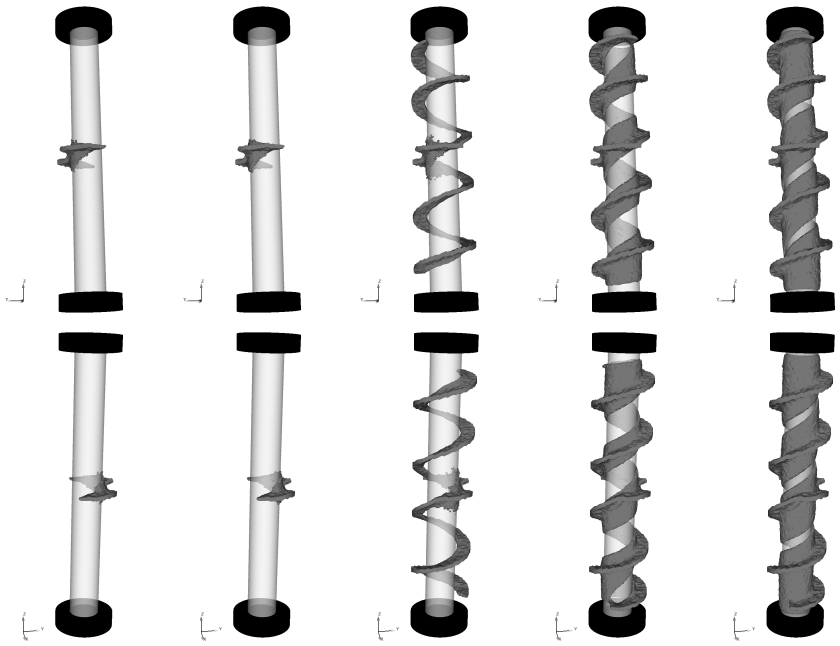

Fig. 3. Traction on a cylinder reinforced in its center. Isovolume $v \leq 5.0\text{E}-2$, representing the crack set at times t =1.5, 1.58, 1.6, 3.08 and 5.5.

the sample. Denoting by α the thermal expansion coefficient of the material, the bulk term of the total energy becomes

$$E^b(u(t^{(p)})) := \frac{1}{2}\int_\Omega A\mathbf{e}(u) : \mathbf{e}(u) - 2\frac{\alpha E}{1-\nu}\theta(t^{(p)};x)\text{tr}\mathbf{e}(u)\,dx, \qquad (11)$$

and the regularized functional E_ε becomes:

$$E_\varepsilon(u,v) := \frac{1}{2}\int_\Omega \left(v^2+\eta_\varepsilon\right)\left(A\mathbf{e}(u) : \mathbf{e}(u) - 2\frac{\alpha E}{1-\nu}\theta(t^{(p)};x)\text{tr}(\mathbf{e}(u))\right)\,dx$$
$$+\gamma\int_\Omega \frac{(1-v)^2}{4\varepsilon} + \varepsilon|\nabla v|^2\,dx. \qquad (12)$$

The numerical implementation is similar to that described above. One major difference, is that unless temperature field depends linearly on the time (which is not the case in the experiments presented farther), the backtracking algorithm cannot be used.

Using this model, we conducted numerical simulations of a glass quenching experiments described in [26, 1, 27, 25]. We consider a thin microscope slide of width 25mm and height 75mm, with elastic moduli E=72.3GPa and $\nu = .23$ and thermal extension parameter α=7.7E-6 K^{-1}, pre-notched in its lower

end. The slide is heated up at temperature θ_H and quenched in a liquid at temperature θ_C at speed $v = 5\text{mm.s}^{-1}$. The temperature difference between the slide and the water bath is $\Delta\theta := \theta_H - \theta_C = 125\text{K}$. Neglecting the effect of the crack on the thermal properties of the sample, the temperature field in the domain is given by

$$\theta(x,y) = \begin{cases} \theta_C \text{ if } y \le vt \\ \theta_C + \Delta\theta e^{\left(-\frac{v}{\kappa}(x-vt)\right)} \text{ otherwise,} \end{cases}$$

where κ is the heat diffusion coefficient. In [25], several experiments are presented for various values of $\Delta\theta$ and v. The qualitative results are as follow, for a given $\Delta\theta$. Below a critical speed v_0, a single crack propagate along the symmetry axis. When $v_0 \le v_1$ for some v_1, the crack starts developing oscillations, then becomes unstable. For $v \ge v_1$, the behavior is more complicated and qualified of "erratic". The crack splits and each branch can in turn propagate a long a straight line, oscillate or branch. For technical reasons, we piloted our numerical experiments in terms of the fracture toughness and thermal conductivity of the material. Up to a rescaling, this is equivalent to varying the temperature difference and quenching speed. Figure 4 represents the final crack pattern for various values of γ and κ. The domain was discretized in 34,736 triangular linear elements and 17,637 nodes. The parameters ε and η_ε are respectively equal to 5E-4 and 1E-7.

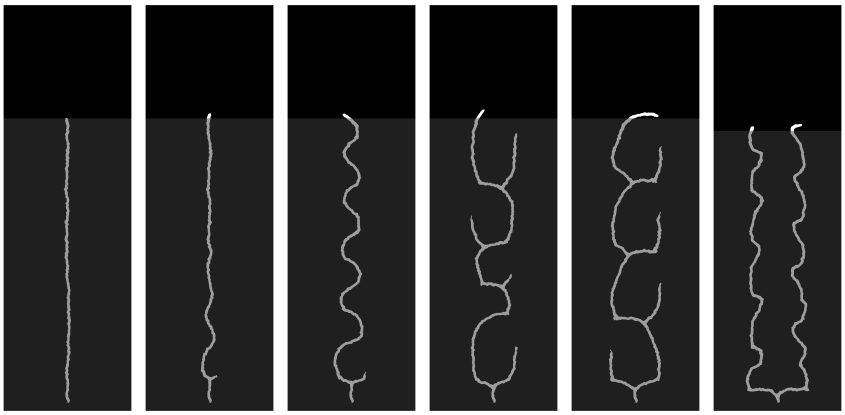

Fig. 4. Quenching of a microscope slide, the v–field for $\kappa = 17.73$ and $\gamma = 12.8, 10.0, 8.8, 7.1$ (left to right in N.m^{-1}), and $\kappa = 10$, $\gamma = 6.0$ (extreme right).

Qualitatively, the results correspond to the behavior depicted in the literature. However, in order to achieve meaningful results, we had to set κ to an unphysical high value (the real value of κ is at least two order of magnitudes lower). Using the actual value, we were only able to obtain "erratic"

propagation, unless the fracture toughness was in turn set to unrealistic high values.

Several hypothesis that could already explain this, but the problem is still open. Since the backtracking algorithm does not apply to this problem, we have no guaranty that the numerical results correspond to global minimizers. Conversely, it may be possible that the actual physical solution may be a *local* and not *global* minimizer of E_ε.

5 Conclusion and extensions

The numerical experiments presented here illustrate some the strength of the Francfort-Marigo approach, but also some pending issues with the model as well as its numerical implementations.

Beside the model's ability to predict crack path, as well as position along this path, one of the strength of Francfort and Marigo's model resides in its being applicable in two and three spaces dimensions without any modification. Indeed, none of the difficulties involved in the three–dimensional numerical implementation are related to the model itself. Instead, the major issues are the usual ones in three dimensional finite elements, *i.e.* mesh generation, visualization, file formats, or size of the discrete models, for instance.

Also, by representing the cracks in terms of the function v in (7), one avoids all difficulties related to the parameterisation of potentially complicated curves or surfaces. Note how the cracks in Figure 3 would be complicated to represent in terms of an explicit function, and how in Figure 4, simple or branched cracks are represented without special treatment. Also, again because of this representation, branching or splitting of cracks requires no special treatment to be represented.

Of course, these benefits are obtained at the cost of theoretical and numerical difficulties. In the numerical experiments and the description of the model, we had to limit the type of body forces we consider. Indeed, the formulation in its current state is inherently unable to handle surface or body forces applied to a brittle material (see the discussion in [19]). Another issue resides in the use of a Griffith-based criterion to render crack initiation and propagation simultaneously. Using cohesive energies *à la* Barenblatt may be more sound, however, the mathematical difficulties involved in doing so are tremendous and far from being solved at this point.

At the numerical level, global minimization is also very involving, as the energy to be minimized is non-convex. Future numerical work will include investigation of better minimization algorithms, as well as the study of the stability of critical points, using the Hessian of E_ε. See for that matter the analytical study of the stability of the local minimizer for a traction problem on a long beam in [8]. Lastly, numerical and mathematical evidences also suggest that in some cases, global minimization may lead to unphysical evolutions.

Alternate models involving local minimization may address that issue in the future.

Acknowledgements

Support for this work was provided by the Louisiana Board of Regents grant LEQSF (2003-06)-RD-A-05 and the National Science Foundation grant DMS-0605320. Parts of the numerical experiments were performed using the National Science Foundation TeraGrid resources provided by NCSA and PSC under the Development Allocation TG-DMS060007T and the Medium Resource Allocation TG-DMS060011N.

References

1. M. Adda-Bedia and Y. Pomeau. Crack instabilities of a heated glass strip. *Phys. Rev. E*, 52(4):4105–4113, 1995.
2. G. Alberti. Variational models for phase transitions, an approach via Γ–convergence. In G. Buttazzo *et al.*, editor, *Calculus of Variations and Partial Differential Equations*, pages 95–114. Springer–Verlag, 2000.
3. L. Ambrosio and V.M. Tortorelli. Approximation of functionals depending on jumps by elliptic functionals via Γ-convergence. *Comm. Pure Appl. Math.*, 43(8):999–1036, 1990.
4. L. Ambrosio and V.M. Tortorelli. On the approximation of free discontinuity problems. *Boll. Un. Mat. Ital. B (7)*, 6(1):105–123, 1992.
5. G. Bellettini and A. Coscia. Discrete approximation of a free discontinuity problem. *Numer. Funct. Anal. Optim.*, 15(3-4):201–224, 1994.
6. B. Bourdin. *Une méthode variationnelle en mécanique de la rupture, théorie et applications numériques*. PhD thesis, Université Paris Nord, Institut Galilée, France, 1998. available from `http://www.math.lsu.edu/~bourdin`.
7. B. Bourdin. Image segmentation with a finite element method. *M2AN Math. Model. Numer. Anal.*, 33(2):229–244, 1999.
8. B. Bourdin. Numerical implementation of a variational formulation of quasi-static brittle fracture. To appear, 08 2006.
9. B. Bourdin and A. Chambolle. Implementation of an adaptive finite-element approximation of the Mumford-Shah functional. *Numer. Math.*, 85(4):609–646, 2000.
10. B. Bourdin, G.A. Francfort, and J.-J. Marigo. Numerical experiments in revisited brittle fracture. *J. Mech. Phys. Solids*, 48(4):797–826, 2000.
11. A. Braides. *Γ-convergence for beginners*, volume 22 of *Oxford Lecture Series in Mathematics and its Applications*. Oxford University Press, Oxford, 2002.
12. A. Chambolle. An approximation result for special functions with bounded variations. *J. Math Pures Appl.*, 83:929–954, 2004.
13. A. Chambolle. Addendum to "an approximation result for special functions with bounded deformation" [j. math. pures appl. (9) 83 (7) (2004) 929–954]: the n-dimensional case. *J. Math Pures Appl.*, 84:137–145, 2005.

14. A. Chambolle, A. Giacomini, and M. Ponsiglione. Crack initiation in elastic bodies. To appear, 2005.
15. G. Dal Maso. *An introduction to Γ-convergence*. Birkhäuser, Boston, 1993.
16. G. Dal Maso, G.A. Francfort, and M. Toader. Quasi-static evolution in brittle fracture: the case of bounded solutions. In *Calculus of variations: topics from the mathematical heritage of E. De Giorgi*, volume 14 of *Quad. Mat.*, pages 245–266. Dept. Math., Seconda Univ. Napoli, Caserta, 2004.
17. G.A. Francfort and C. Larsen. Existence and convergence for quasi-static evolution in brittle fracture. *Comm. Pure Appl. Math.*, 56(10):1465–1500, 2003.
18. G.A. Francfort and J.-J. Marigo. Revisiting brittle fracture as an energy minimization problem. *J. Mech. Phys. Solids.*, 46(8):1319–1342, 1998.
19. G.A. Francfort and J.-J. Marigo. Griffith theory of brittle fracture revisited: merits and drawbacks. *Latin American J. Solids Structures*, 2005.
20. A. Giacomini. Ambrosio-Tortorelli approximation of quasi-static evolution of brittle fractures. *Calc. Var. Partial Differential Equations*, 22(2):129–172, 2005.
21. Alessandro Giacomini and Marcello Ponsiglione. A discontinuous finite element approximation of quasi-static growth of brittle fractures. *Numer. Funct. Anal. Optim.*, 24(7-8):813–850, 2003.
22. L. Modica and S. Mortola. Il limite nella Γ–convergenza di una famiglia di funzionali ellittici. *Boll. Un. Mat. Ital. A (5)*, 14(3):526–529, 1977.
23. L. Modica and S. Mortola. Un esempio di Γ^-–convergenza. *Boll. Un. Mat. Ital. B (5)*, 14(1):285–299, 1977.
24. M. Negri. A finite element approximation of the Griffith model in fracture mechanics. *Numer. Math.*, 95:653–687, 2003.
25. B. Yang and K. Ravi-Chandar. Crack path instabilities in a quenched glass plate. *J. Mech. Phys. Solids*, 49:91–130, 2000.
26. A. Yuse and A.M. Sano. Transition between crack patterns in quenched glass plates. *Nature*, 362:329–330, 1993.
27. A. Yuse and M. Sano. Instability of quasi-static crack patterns in quenched glass plates. *Physica D*, 108:365–378, 1997.